A Handy and Accessible Tool for Identification of Sn(II) in Toothpaste: Inclination to an Eco-Friendly Environment

Shampa Kundu
Visva-Bharati University
Khai-Nghi Truong
University of Jyvaskyla
Shrabani Saha
Visva-Bharati University
Kari Rissanen
University of Jyvaskyla
Prithidipa Sahoo (prithidipa@hotmail.com)
Visva-Bharati University

Research Article

Keywords: accessible, identification, toothpaste, Inclination, eco-friendly environment, colorimetric probe, sensing mechanism, Selective detection

Posted Date: December 9th, 2021

DOI: https://doi.org/10.21203/rs.3.rs-1137051/v1

Abstract

An easily accessible colorimetric probe, a carbazole-naphthaldehyde conjugate (**CNP**), was successfully prepared for the selective and sensitive recognition of Sn(II) in different commercially-available toothpaste and mouth wash samples. The binding mechanism of **CNP** for Sn^{2+} was confirmed by UV-Vis, ^{1}H and ^{13}C NMR titrations. The proposed sensing mechanism was supported by quantum chemical calculations. Selective detection of Sn(II) in the nanomolar range (85 nM), among other interfering metal ions, makes it exclusive. Moreover, Sn^{2+} can be detected with a simple paper strip from toothpaste, which makes this method handy and easy accessible. The potential application of this system for monitoring Sn^{2+} can be used as an expedient tool in environmental and industrial purpose.

Introduction

The utilization of tin has been established for thousands of years and is most commonly used for the manufacturing of bronze, which is a tin and copper alloy. In recent era, Sn(II) is used in many fields in industry such as aerospace, construction and home decor, electronics, jewelry manufacturing, telecommunications, paint/plastic industries and agriculture via pesticides.[1] Sn(II) as fluoride is present in a number of dental care products such as toothpaste and mouth rinse. Sn^{2+} has been utilized in dentistry as a chemical adjunct to prevent dental caries since the 1950s.[2] Sn^{2+} was found to effectively inhibit Streptococcus mutants, which leads to tooth decay in human inter proximal dental plaque and oral disease.[3] However, wide utilization of toothpaste in our everyday life may increase the consumption of Sn^{2+} in human body. The continuous use of Sn(II) becomes detrimental for our health and environment as well. The uprising of the climate change, people's views of toothpaste have changed nowadays. Why is toothpaste targeted and how bad is it really for the environment? Humans can intake Sn(II) by breathing, by the skin, by the consumption of food.[4] The accumulation of Sn(II) can induce acute and long-term effects in the human body. The acute effects are eye irritations, heavy sweating and urination complications. The long-term effects include disorders in the immune system, damage in liver functioning, chromosomal destruction, damage in the brain, and lack of red blood cells.[5] Moreover, accumulation of excess amounts of Sn(II) can damage live cells, which would lead to inhibited zinc metabolism, causing severe illness in both lung and gastric systems.[6] Excess consumption of Sn(II) also finds severe immunotoxic and neurotoxic effects in human causing symptoms, generally gastrointestinal complaints, such as diarrhea, vomiting, nausea and cramps.[7] Recent studies revealed that the presence of an excess of Sn(II) in humans can easily be coordinated by white blood cells and enter into the cells by calcium channels, inducing DNA damage.[8] According to the guiding principles of World Health Organization's (WHO) for metals, the permissible limit of Sn(II) in drinking water and canned foods are 8.4×10^{-4} M to 8.4×10^{-3} M and 2.105×10^{-6} M, respectively.[9] Due to the hazardous impacts of Sn(II) to humans, consumption of Sn(II) must be closely monitored.

In literature, several modern analytical methods are available for detection of Sn^{2+} ion such as ion-exchange chromatography,[10] atomic absorption spectroscopy,[11] electrochemical methods,[12–13] flow injection,[14] adsorptive stripping voltammetry,[15] and liquid chromatography.[16] Nevertheless, these methods are accompanied by many drawbacks i.e. high operational cost, complicated sample handling, use of harmful solvents, time-consuming, require sophisticated equipment, trained operators. The development of highly sensitive expedient and readily accessible tool is the greatest requirement. Colorimetric sensing method is one of the simplest and convenient sensing methods over other established detection techniques because it offers the advantage of 'on spot' real time detection with naked eyes, low cost, portable, and wide applicability.[17–25] Hence, inspired with the requirement of active colorimetric probes, herein, we report the synthesis and sensing behavior of a novel colorimetric probe carbazole-naphthaldehyde conjugate (**CNP**) that exhibits high selectivity and sensitivity toward Sn^{2+} in neutral aqueous medium (10 mM phosphate buffer, pH =7.0). The structure of the synthesized probe **CNP** was confirmed by detailed NMR (^{1}H NMR, ^{13}C NMR), HRMS, and X-ray analysis (Figure S1-S4, ESI†) as well as optimised by density functional theory. Single crystals suitable for X-ray diffraction were obtained by slow evaporation of an acetonitrile solution of **CNP** at 3°C. It crystallises in the monoclinic space group $P2_1/n$ (Figure 1, Figure S4 in ESI†). Different than in solution where **CNP** is unequivocally present as the enol-imine tautomer (Figure S1 and S2 in ESI†), the X-ray structure of **CNP** revealed that the compound is in the keto-enamine form in solid-state. The probe **CNP** displayed higher selectivity toward Sn^{2+}, whereas the interference of the coexisting metal ions was strictly inhibited. Moreover, the probe presented a good limit of detection (LOD), association constant (K_a), and rapid response in the aqueous medium. Significantly, the discriminative detection and quantification of Sn^{2+} in different toothpaste samples has also been accomplished using our synthesized probe **CNP**. To the best of our knowledge, this is the first colorimetric sensor displaying a distinguished recognition of Sn^{2+} in different toothpaste and mouth wash samples.

Results And Discussions

To explore the interaction pattern of the probe **CNP** with Sn^{2+}, we have performed several experiments such as NMR titration, absorbance titration, pH titration, selectivity test and theoretical calculations.

NMR Titration Analysis

Interactive properties of the probe **CNP** towards Sn^{2+} was investigated through ^{1}H, ^{13}C NMR titrations in DMSO-d_6 and D_2O. In ^{1}H NMR titration, the aromatic -OH proton peak at 16.37 ppm abruptly disappears after addition of one equivalent of Sn^{2+} ($SnCl_2$ dihydrate), followed by downfield shift of imine proton peak at 9.84 ppm. This phenomena indicates the formation of strong coordination between -OH, -N groups of **CNP** and Sn^{2+} (Figure S5, ESI†). Moreover in ^{13}C NMR titration with the addition of one equivalent Sn^{2+}, the carbon attached with -OH group shifts downfield from 169 ppm to 193 ppm and also

the imine 'C' peak at 153 ppm shifted towards 159 ppm with decreased intensity (Figure S6, ESI†). The above features also confirm the formation of **CNP-Sn^{2+}** complex.

UV-Vis spectral behaviour of CNP with Sn^{2+}

The interactions between the probe **CNP** and Sn^{2+} was demonstrated by absorbance titration in acetonitrile:water (1:8, v/v) at neutral pH value (pH 7.0, 10 mM phosphate buffer). In the UV–Vis absorption spectra, we get a characteristic absorbance peak of **CNP** at 400 nm which decreases upon incremental addition of Sn^{2+}, with an enhancement at 454 nm followed by a rapid colour change from pale yellow to deep orange. Furthermore, a notable isosbestic point at 425 nm indicates possible stronger interaction between **CNP** and Sn^{2+} (Figure 2a). Ratiometric changes in absorbance with increasing concentration of Sn^{2+} have been represented in Figure 2b.

Binding interactions determine 1:1 stoichiometric ratio of **CNP** and Sn^{2+} (Figure S7, ESI†) with a high association constant of 0.35×10^{6} M^{-1} from absorption spectra[26, 27] (Figure S8, ESI†). The detection limit of **CNP** for Sn^{2+} has been evaluated 0.85 nM (Figure S9, ESI†).

Effect of pH value

pH titration clearly reflects that **CNP** is slight sensitive towards acidic pH values whereas the **CNP-Sn^{2+}** complex is pH independent (Figure S10, ESI†). So, we carried out all the experiments in the pH value range of 7.0 using 10 mM phosphate buffer.

Colorimetric responses of CNP toward various metal ions

The colorimetric behaviour of the sensor probe **CNP** was evaluated upon the addition of various metal ions in the aqueous medium (10 mM phosphate buffer, pH = 7.0). As depicted in Figure S11, the pale yellow color of the probe turned to deep orange with the addition of Sn^{2+}. The synthesized probe **CNP** did not show any notable color changes with the addition of other metal ions. The specific color change of **CNP** with Sn^{2+} was attributed to several electron transitions in the **CNP-Sn^{2+}** complex such as π to π*, d–d, ligand–metal charge transfer, and metal–ligand charge-transfer effects. Furthermore, the comparative spectrophotometric response of **CNP** was also studied with these metal ions which confirms that our probe **CNP** selectivity sense Sn^{2+} over other metal ions (Figure S12, ESI†). Therefore, these experimental results indicate that our synthesized probe **CNP** shows remarkable selectivity and sensitivity towards Sn^{2+} over other analytes which could be a beneficial tool for practical approach.

Theoretical Calculations

Theoretical calculations were executed for **CNP** and **CNP–Sn^{2+}** complex systems using quantum chemical calculations at the DFT level LANL2DZ/6-31G** method basis set implemented at Gaussian 09 program[28] and CPCM (Conductor like Polarizable Continuum Model) solvent model was used for solvent (water) effect incorporation. In the optimized structure of **CNP**, the positions of carbazole and naphthaldehyde units were nearly in the same plane. The optimized structure of the **CNP–Sn^{2+}** complex

showed the formation of coordination bonds of Sn^{2+} with −OH and −N groups of **CNP**, which enhanced the stability of the complex (Figure S13, Table S1, ESI†).

From TDDFT calculation, we can see that there is a sharp S_0-S_1 transition in **CNP** at 410 nm (oscillator strength f = 0.5188) which is very close to that experimentally observed value at 400 nm, responsible for the absorption of the carbazole moiety. Moreover, in **CNP-Sn^{2+}**, the transition at 448 nm (S_0-S_1, f = 0.3563) indicates the π-π* electronic transition from the carbazole to naphthaldehyde moiety which is distinctly executed in the absorbance graph at 454 nm (Table S2, ESI†). Next, the energy distributions of HOMO and LUMO for **CNP** and its Sn^{2+} complex were examined (Table S3, ESI†). As shown in Figure 3, the energy of the HOMO and LUMO orbital levels for the **CNP–Sn^{2+}** complex is lower than that of the probe **CNP**. Also, the HOMO-LUMO energy gap of **CNP** and **CNP–Sn^{2+}** complex was calculated with an energy difference of 0.29 eV.

These outcomes indicate that the effective resonance attraction obtained in the **CNP–Sn^{2+}** complex. The density of the orbital coefficient migrates from the carbazole unit to naphthaldehyde units in **CNP**, whereas in the **CNP–Sn^{2+}** complex, the orbital coefficient of total framework is moving towards Sn^{2+} via N–Sn^{2+} coordination bond. Hence, the obtained results imply the formation of a stable complex, which is consistent with the proposed binding mechanism. Furthermore, the mass of the **CNP–Sn^{2+}** complex has been checked which truly validated the binding mechanism (Figure S14, ESI†). The anticipated coordination mechanism of the **CNP–Sn^{2+}** complex is given in Figure 4. In ^{1}H NMR spectrum, the resonances assigned to the hydroxyl and imine groups are 16.37 ppm and 9.84 ppm, respectively. The naphthalene CO and imine C resonances in ^{13}C NMR spectroscopy are observed at 169.46 and 153.90 ppm, respectively.

Plausible mechanism and explanation.

The naphthalene C-O bond length (1.282(3) Å) observed in the X-ray structure is characteristic of ketones rather than phenols, and the C-N bond (1.324(3) Å) is elongated relative to that of a typical imine. Moreover, the hydrogen atom involved in hydrogen bonding were located on the nitrogen atom rather than on the oxygen atom. In consequence, the pale yellow colour of **CNP** becomes the deep orange colour due to the non-covalent interactions of **CNP** with Sn^{2+} (Figure 4).

Quantitative analysis

The excellent photophysical properties of the probe **CNP** toward Sn^{2+}, such as high sensitivity and selectivity at physiological pH encouraged us to further evaluate the potential of the probe for realistic approach. The specific and selective recognition of Sn^{2+} by the chemosensor **CNP** was also examined in three different toothpaste samples. In this work, we took commercially available toothpastes from three different brands (T1, T2, T3). The details procedure of the preparation of toothpaste solutions was described in ESI†. Toothpaste solutions were then added to the **CNP** solution, a rapid orange color change resulted after few minutes (Figure 5a). Furthermore, the method was also applied to recognize Sn^{2+} by a

simple paper strip in different toothpaste solutions. Three paper strips soaked in **CNP** were dipped separately in the different toothpaste solutions (T1, T2, T3), and Figure 5b shows the respective color changes of **CNP**-coated paper strip after dipping in the toothpaste solutions T1, T2, T3 respectively.

The concentration of Sn^{2+} was also quantified from these three different toothpaste samples (T1, T2, T3). For this work, the above-mentioned toothpaste samples were subjected to colorimetric analysis at pH 7.0 (10 mM phosphate buffer) to quantify the amount of Sn^{2+} present therein. Sn^{2+} was quantified from these given samples by **CNP** (1 μM) by virtue of its selective and direct recognition properties. All estimations were done in triplicate. Concentrations of Sn^{2+} were estimated by comparison with the **CNP-Sn^{2+}** standard absorbance curve. From the standard curve it was found that the concentration of Sn^{2+} were 0.73 μM, 0.70 μM and 0.64 μM in 100 μL of T1, T2 and T3 samples, respectively (Figure 6, Table 1). Concentration of Sn^{2+} was further quantified from two different mouth wash samples (M1, M2) using above mentioned procedure and the respective values are 0.25 μM and 0.28 μM in 100 μL sample solution (Table 2).

Conclusion

In conclusion, a new carbazole-naphthaldehyde based colorimetric probe **CNP** was successfully synthesized for selective recognition of Sn^{2+} in the aqueous medium under physiological pH value. The structure of the synthesized probe **CNP** was analyzed by single crystal X-ray diffraction, ^{1}H and ^{13}C NMR spectroscopy as well as mass spectrometry (HRMS). The sensing mechanism has been triggered by the strong coordination bonding of-groups with Sn^{2+}, which was confirmed by spectroscopic investigations. Theoretical calculations were also performed to justify the binding mechanism and optical behavior of the sensor probe. **CNP** showed high selectivity and sensitivity for Sn^{2+} even in the presence of other metal ions. The detection limit of the probe for Sn^{2+} was calculated to be 85 nM, which is much lower than WHO permissible amount of Sn^{2+} in drinking water. We further demonstrated that **CNP** has been utilized as a colorimetric sensor to detect and quantify trace amounts of Sn^{2+} in different toothpaste and mouth wash samples. Being a potential probe, it can be used as an expedient ‘in-field’ approach to estimate Sn^{2+} in environmental and industrial purpose for a sustainable and environment-friendly industrial production.

Experimental Section

Materials and methods. All the reagents were purchased from Sigma-Aldrich Pvt. Ltd. (India). Unless otherwise mentioned, materials were obtained from commercial suppliers and were used without further purification. Solvents were dried according to standard procedures. Elix Millipore water was used in all respective experiments. ^{1}H and ^{13}C NMR spectra were recorded on a Bruker 400 MHz instrument. For NMR spectra, DMSO-d_6 and for NMR titration DMSO-d_6 and D_2O were used as solvent using TMS as an internal standard. Chemical shifts are expressed in δ ppm units and $^{1}H–^{1}H$ and $^{1}H–^{13}C$ coupling constants in Hz. The mass spectrum (HRMS) was carried out using a micromass Q-TOF Micro™

instrument by using methanol as a solvent. Fluorescence spectra were recorded on a PerkinElmer Model LS55 spectrophotometer. UV spectra were recorded on a SHIMADZU UV-3101PC spectrophotometer. The following abbreviations are used to describe spin multiplicities in ^{1}H NMR spectra: s = singlet; d = doublet; t = triplet; m = multiplet. Single crystal X-ray data of **CNP** was measured using a dual-source Rigaku Super Nova diffractometer equipped with an Atlas detector and an Oxford Cryostream cooling system using mirror-monochromated Cu-K_α radiation (λ = 1.54184 Å). Data collection and reduction for both compounds were performed using the program *CrysAlisPro*[29] and Gaussian face-index absorption correction method was applied.[29] The structures were solved with Direct Methods (*SHELXS*)[30–32] and refined by full-matrix least-squares based on F^2 using *SHELXL*-2015.[30–32] Non-hydrogen atoms were assigned anisotropic displacement parameters unless stated otherwise. The hydrogen atom bonded to nitrogen was located from Fourier difference maps and refined with an N–H distance restraint of approximately 0.96 Å. Otherhydrogen atoms were placed in idealised positions and included as riding. Isotropic displacement parameters for all H atoms were constrained to multiples of the equivalent displacement parameters of their parent atoms with U_{iso}(H) = 1.2 U_{eq}(parent atom). The single crystal X-ray data, experimental details as well as CCDC number are given in the Supporting Information.

Synthetic procedure of CNP: In a 100 ml round bottom flask, 2-hydroxy naphthaldehyde (1.0 g, 5.8 mmol) in 30 ml ethanol was vigorously stirred at ambient temperature for few minutes. Then, 3-amino-9-ethyl carbazole (1.46 g, 6.95 mmol) was dissolved in ethanol (10 mL) and added dropwise to the solution. The reaction mixture was refluxed for 24 hours at 83°C. After completion of the reaction (monitored by TLC), the solvent was evaporated completely under reduced vapor pressure, then extracted with chloroform and water. After drying it over anhydrous Na_2SO_4, the organic layer was evaporated completely to get the solid product. This product was purified by column chromatography with the eluent $CHCl_3$:PET (5:1, v:v) to get the product **CNP** with 86% yield (Figure 7). ^{1}H NMR (400 MHz, DMSO-d_6): δ (ppm) = 16.37 (s, 1H), 9.84 (s, 1H), 8.57-8.59 (d, 2H, J=8Hz), 8.26-8.28 (d, 1H, J=8Hz), 7.90-7.92 (d, 1H, J= 8Hz), 7.77-7.82 (t, 2H, J=20Hz), 7.71-7.73 (d, 1H, J=8Hz), 7.62-7.64 (t, 1H, J=8Hz), 7.55-7.57 (t, 1H, J=8Hz), 7.47-7.51 (t, 1H, J=16Hz), 7.34-7.37 (t, 1H, J=12Hz), 7.23-7.26 (t, 1H, J=12Hz), 7.04-7.06 (d, 1H, J=8 HZ), 4.47-4.49 (q, 2H, J=8Hz), 1.31-1.34 (t, 3H, J=12Hz). ^{13}C NMR (100 MHz, DMSO-d_6): δ (ppm)= 169.46, 153.90, 140.30, 138.46, 135.94, 133.15, 129.04, 127.93, 126.67, 126.32, 123.28, 123.02, 122.26, 122.11, 120.92, 120.36, 119.55, 119.05, 112.08, 109.98, 109.52, 108.67, 37.19, 13.83. HRMS (TOF MS): (m/z, %): Calcd. for $C_{25}H_{20}N_2O$: 364.1576. Found: m/z = 365.1283 ($M+H^+$).

Declarations

Author contributions

S.K. performed all the experiments, interpreted data and prepared the manuscript.

K.-N.T. and K.R. helped with the crystallographic analysis and revision of the manuscript.

S.S. cross checked the manuscript and supporting information thoroughly and modified several sections.

P.S. conceptualised the research, designed the experiments, wrote and edited the manuscript.

CONFLICTS OF INTEREST

There are no conflicts to declare.

ASSOCIATED CONTENT

^{1}H NMR, ^{13}C NMR, and MS spectra, experimental section, additional spectroscopic data, supplementary fluorescence images, theoretical calculation tables.

ACKNOWLEDGMENT

P.S. acknowledges CSIR, India, for awarding her the major grant [Project file no. 02(0384)/19/EMR-II dated 20/05/2019]. S.K. and S.S. is sincerely thankful to UGC India for her research fellowship.

References

1. Ravichandiran, P. *et al.* Naphthoquinone-Dopamine Linked Colorimetric and Fluorescence Chemosensor for Selective Detection of Sn. *Ion in Aqueous Medium and Its Bio-Imaging Applications. J. ACS Sustainable Chem. Eng*, **8**, 10947–10958 https://doi.org/10.1021/acssuschemeng.0c03548 (2020).
2. Special issue, Tinanoff, N.Int. J. Clin. Dent., 6,37(1995)
3. Keene, H. J., Shklair, I. L. & Mickel, G. J. Effect of multiple dental floss-SnF_2 treatment on Streptococcus mutans in interproximal plaque. *J. Dent. Res*, **56**, 21 (1977).
4. Ravichandiran, P. *et al.* Simple Colorimetric and Fluorescence Chemosensing Probe for Selective Detection of Sn^{2+} Ions in an Aqueous Solution: Evaluation of the Novel Sensing Mechanism and Its Bioimaging Applications. *Anal. Chem*, **93**, 801–811 (2021).
5. Rudel, H. Case study: bioavailability of tin and tin compounds. *Ecotoxicol. Environ. Saf*, **56**, 180–189 (2003).
6. Lan, H. *et al.* Fluorescence turn-on detection of Sn^{2+} in live eukaryotic and prokaryotic cells. *Analyst*, **139**, 5223–5229 (2014).
7. Cardarelli, N. Tin and the thymus gland: a review. *Thymus*, **15**, 223–231 (1990).
8. Sherman, L. R., Masters, J., Peterson, R. & Levine, S. Tin concentration in the thymus glands of rats and mice and its relation to the involution of the gland. *J. Anal. Toxicol*, **10** (1), 6–9 (1986).
9. Jianqiang, W. *et al.* Highly sensitive and selective fluorescent detection of rare earth metal Sn (II) ion by organic fluorine Schiff base functionalized periodic mesoporous material in aqueous solution. *J. Photochem. Photobiol. A*, **309**, 37–46 (2015).

10. Christison, T. T. & Rohrer, J. S. Direct determination of free cyanide in drinking water by ion chromatography with pulsed amperometric detection. *J. Chromatogr. A*, **1155**, 31–39 https://doi.org/doi: 10.1016/j.chroma.2007.02.083. (2007).
11. Dabeka, R. W., McKenzie, A. D. & Albert, R. H. Atomic absorption spectrophotometric determination of tin in canned foods, using nitric acid-hydrochloric acid digestion and nitrous oxide-acetylene flame: collaborative study. *J. Assoc. Off. Anal. Chem*, **68**, 209–213 (1985).
12. Safavi, A., Maleki, N. & Shahbaazi, H. R. Indirect determination of cyanide ion and hydrogen cyanide by adsorptive stripping voltammetry at a mercury electrode. *Anal. Chim. Acta*, **503**, 213–221 (2004).
13. Boutakhrit, K., Yang, Z. P. & Kauffmann, J. M. Inorganic tin(II) determination by FIA with amperometric detection of its oxinate complex. *Talanta*,,1883–1890(1995)
14. Themelis, D. G., Karastogiann, S. C. & Tzanavaras, P. D. Selective determination of cyanides by gas diffusion-stopped flow-sequential injection analysis and an on-line standard addition approach. *Anal. Chim. Acta*, **632**, 93–100 (2009).
15. Heppeler, F., Sander, S. & Henze, G. Determination of tin traces in water samples by adsorptive stripping voltammetry. *Anal Chim Acta*, **319**, 19–24 (1996).
16. Ichinoki, S., Iwase, H., Arakawa, F., Hirano, K. & Fujii, Y. Selective determination of tin(II) ion in water by solventextraction with salicylidenamino-2-thiophenol followed byreversed-phase highperformance liquid chromatographywith photometric detection. *J Liq Chromatogr Relat Technol*, **26**, 3129–3139 (2003).
17. Kundu, S. & Sahoo, P.New J. Chem., 43,12369–12374(2019)
18. Kundu, S., Sarkar, H. S., Das, S. & Sahoo, P.New J. Chem., 43,6843–6847(2019)
19. Sarkar, H. S. *et al.*RSC Adv., 8,39893–39896(2018)
20. Ghosh, A., Das, S., Kundu, S., Maiti, P. & Sahoo, P. K. &Sensors and Actuators B:Chemical, 266,80–85(2018)
21. Kundu, S., Maiti, P. K. & Sahoo, P.Asian J. Org. Chem., 9,94–98(2020)
22. Kundu, S., Saha, S. & Sahoo, P.Results in Chemistry, 1,100014(2019)
23. Ghosh, A., Das, S., Sarkar, H. S., Kundu, S. & Sahoo, P.ACS Omega, 3,11617–11623(2018)
24. Das, S. *et al.*Anal Bioanal Chem., 2019, https://doi.org/10.1007/s00216-019-02012-9
25. Das, S. & Sahoo, P.Sensors and Actuators B:Chemical, 2019, https://doi.org/10.1016/j.snb.2019.04.089.
26. Chunwei, Y. *et al.*Microchim. Acta, 174,247–255(2011)
27. Das, S., Sarkar, H. S., Uddin, M. R., Mandal, S. & Sahoo, P.Sens. Actuators B: Chem, 259,332–338(2018)
28. Frisch, M. J. *et al.* J. V., Cioslowski J. & Fox, D. J. *Gaussian 09, Revision A. 02*, Gaussian, Inc., Wallingford CT, 2009
29. Rigaku, O. D. *Crys Alis Pro software system, version 38.46* (Rigaku Corporation, Oxford, UK, 2017).
30. Sheldrick, G. M. A short history of ShelX. *Acta Cryst*, **A64**, 112–122 (2008).

31. Sheldrick, G. M. *SHELXL13. Program package for crystal structure determination from single crystal diffraction data* (University of Göttingen, Germany, 2013).
32. Sheldrick, G. M. Crystal structure refinement with ShelXL. *Acta Cryst*, **C71**, 3–8 (2015).

Tables

Table 1 Determination of [Sn^{2+}] in algae solutions under UV-lamp

Toothpaste sample	Conc. of CNP (µM)	Amount of toothpaste sample taken (µL)	Conc. of Sn^{2+} (µM)	Average conc. of Sn^{2+}(µM)
T1	1	100	0.73	0.73
		100	0.74	
		100	0.72	
T2	1	100	0.69	0.70
		100	0.70	
		100	0.71	
T3	1	100	0.63	0.64
		100	0.65	
		100	0.64	

Table 2. Determination of [Sn^{2+}] in different mouth wash samples

Mouth wash sample	Conc. of CNP (µM)	Amount of Mouth wash sample taken(µL)	Conc. of Sn^{2+} (µM)	Average conc. of Sn^{2+}(µM)
M1	1	100	0.25	0.25
		100	0.23	
		100	0.24	
M2	1	100	0.29	0.28
		100	0.27	
		100	0.28	

Figures

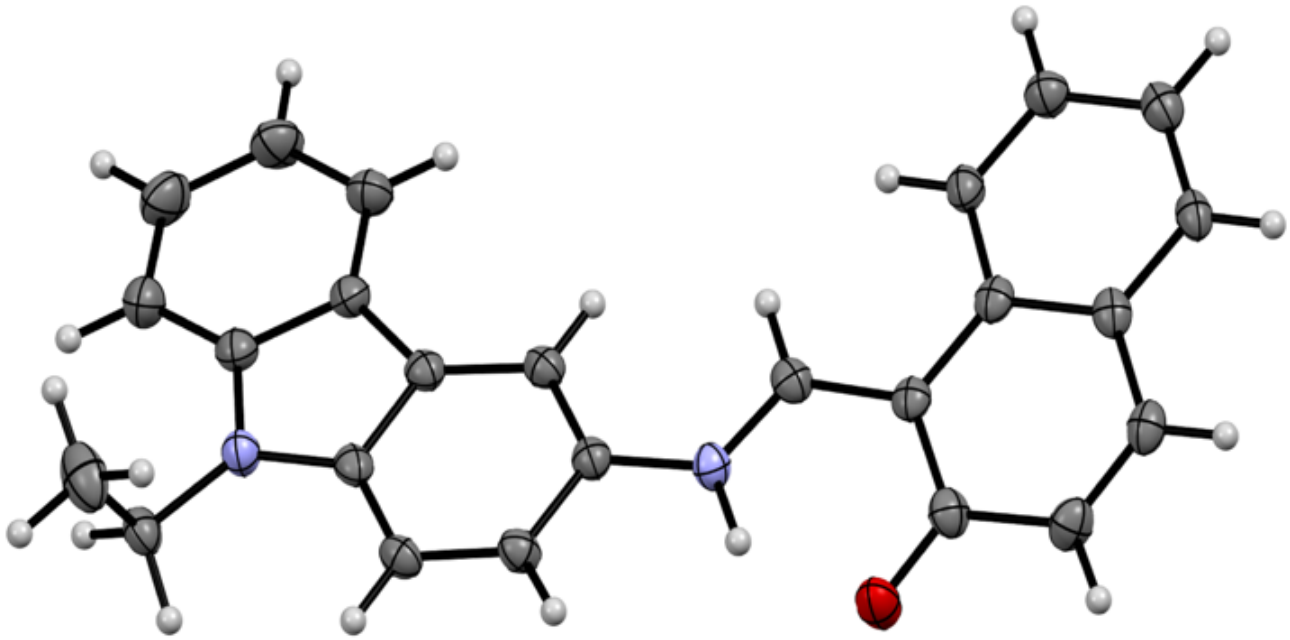

Figure 1

Displacement ellipsoid plot of CNP. Displacement ellipsoids are drawn at the 50% probability level.

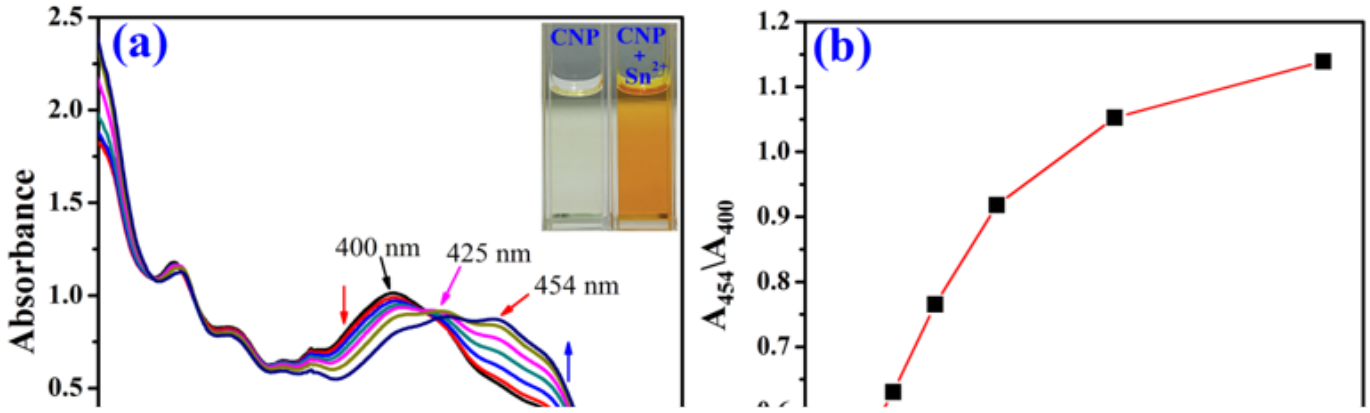

Figure 2

(a) UV–Vis absorption spectra of CNP (1 μM) upon incremental addition of Sn2+ up to 1.2 μM in CH3CN:H2O (1:8, v/v) at pH 7.0 (10 mM phosphate buffer) [Inset: naked eye colour change of CNP on addition of Sn2+]. (b) Ratiometric change in absorbance with increasing concentration of Sn2+ at neutral pH.

Figure 3

HOMO and LUMO distributions of CNP and CNP–Sn2+.

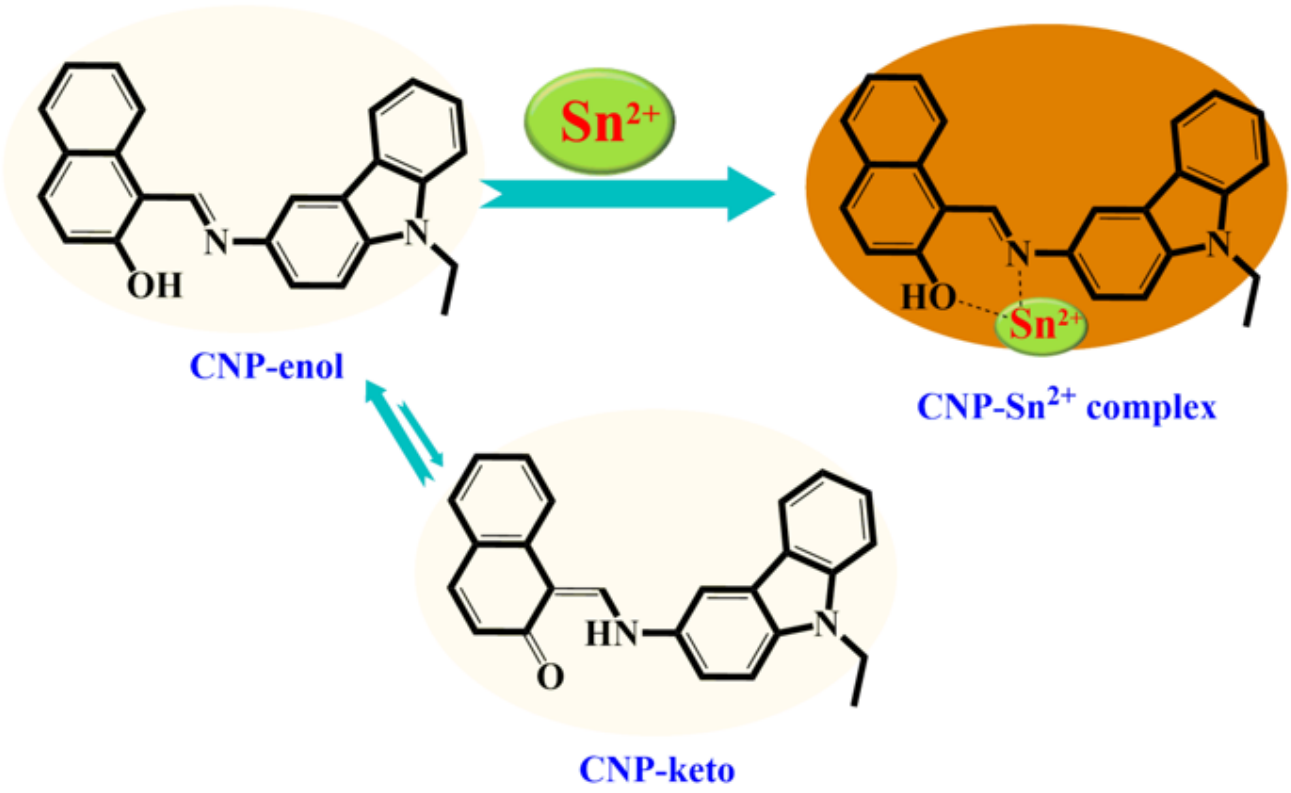

Figure 4

Proposed colorimetric detection mechanism of the CNP-Sn2+ complex.

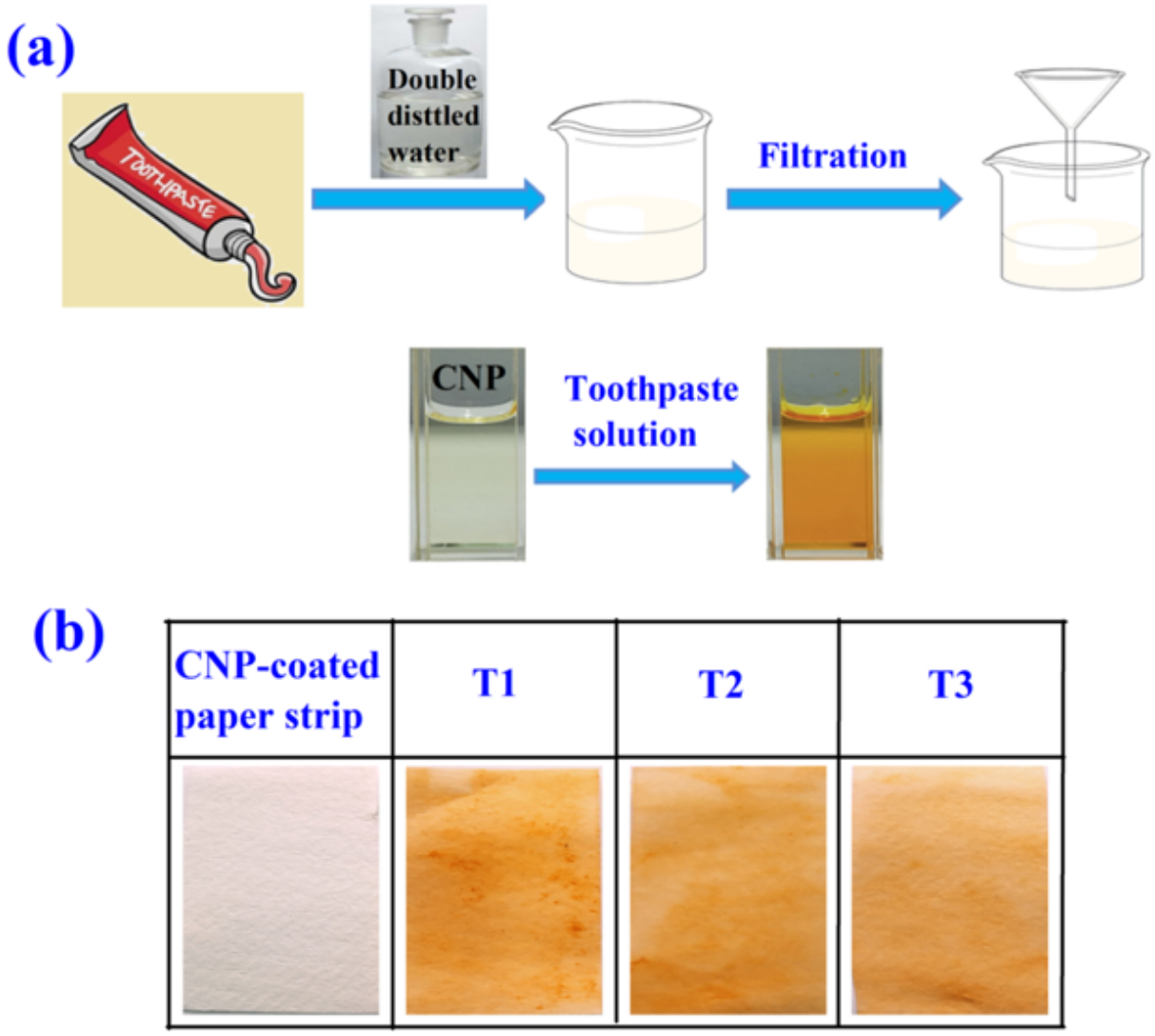

Figure 5

(a) Schematic diagram for estimation of Sn2+ in toothpaste samples using the probe CNP. (b) Display of naked-eye color change of CNP-coated paper strip after dipping in T1, T2, T3 solutions, respectively) (all experiments performed at pH 7.0, 10 mM phosphate buffer).

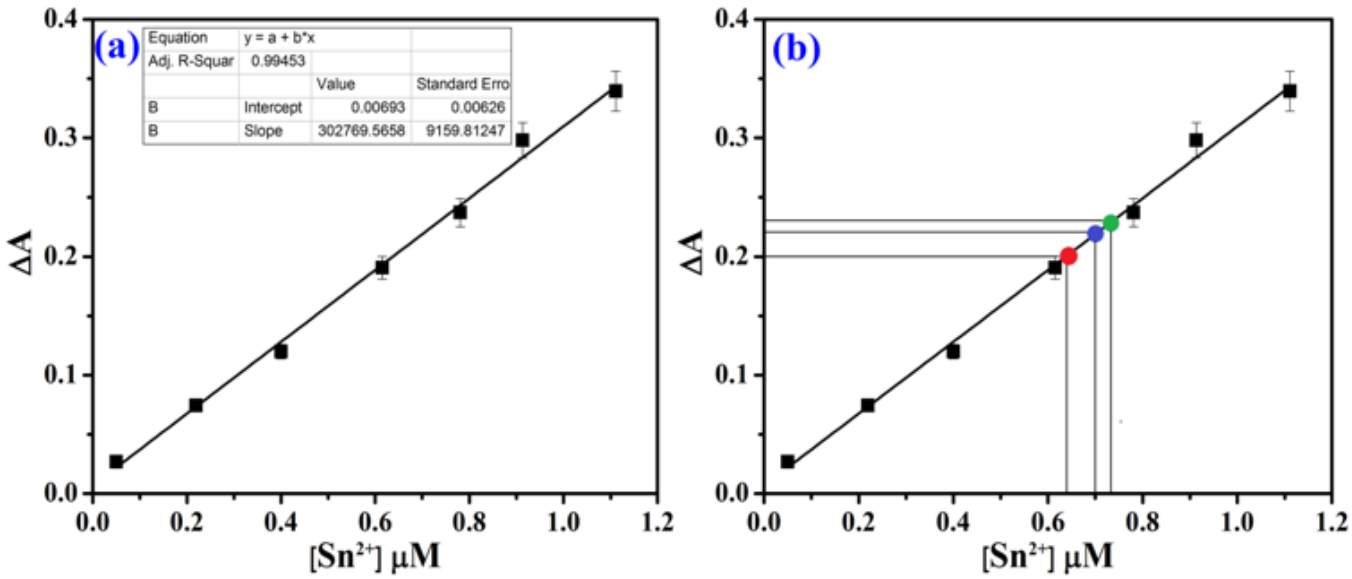

Figure 6

(a) Standard fluorescence curve obtained for the estimation of Sn2+ ions;. (b) Estimation of unknown concentration of Sn2+ ions (red, blue and green point) in the different toothpaste samples from the standard fluorescence curve. Standard deviations are represented by error bar (n = 3).

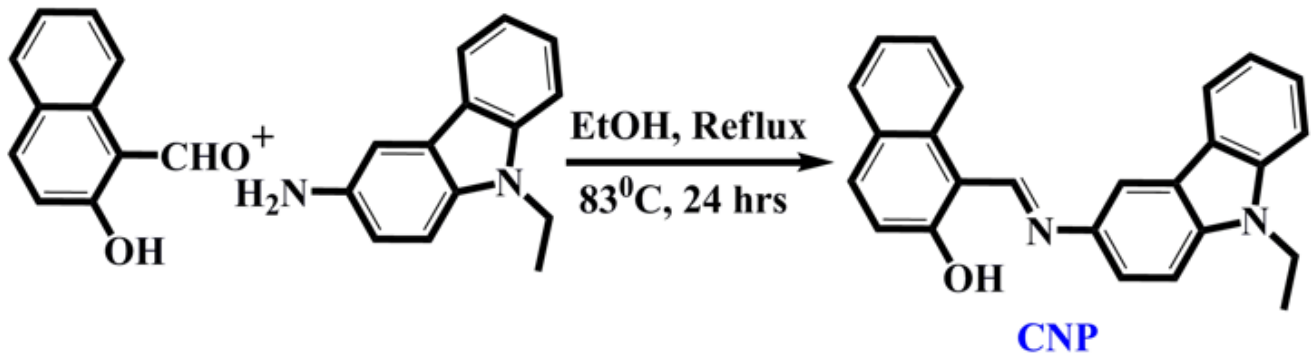

Figure 7

Synthesis of the probe CNP.

Supplementary Files

This is a list of supplementary files associated with this preprint. Click to download.

- SuportingInformation.docx

- Tableofcontent.png